PCCP

Accepted Manuscript

ROYAL SOCIETY OF CHEMISTRY

www.rsc.org/pccp

Journal Name

RSCPublishing

ARTICLE

Experimental evidence of dual emission in a negatively solvatochromic push−pull pyridinium derivative

Cite this: DOI: 10.1039/x0xx00000x

Received 00th January 2012,
Accepted 00th January 2012

DOI: 10.1039/x0xx00000x

www.rsc.org/

B. Carlotti,[a] A. Cesaretti,[a] C. G. Fortuna,[b] A. Spalletti[a] and F. Elisei[a,*]

We report here experimental evidence of dual emission in a cationic push−pull system (bearing a methyl pyridinium group as electron acceptor and a diphenylamino group as electron donor), which shows negative solvatochromism. An intriguing blue shift and enlargement of the fluorescence band upon increasing the solvent polarity have suggested a possible contribution of an upper excited state to the stationary emission. Ultrafast transient absorption has indeed revealed the presence of an intermediate transient species in some solvents. The investigation of the fluorescence properties at low temperatures and in rigid matrix has given clear indication of this additional emission at shorter wavelengths. Femtosecond up-conversion measurements have shown interesting rise−decay dynamics in the kinetics and two well distinguished emission bands characterized by different deactivations. A single isoemissive point in the time−resolved area−normalized spectra has unambiguously pointed out the presence of two consecutive emissive species: the locally excited and the intramolecular charge transfer excited states.

Introduction

Organic compounds bearing electron donor (D) and acceptor (A) groups linked by π conjugated bridges have interestingly shown the occurrence of fast intramolecular charge transfer (ICT) upon light excitation.[1] Dual fluorescence has been observed in some push-pull derivatives, coming from both the initially populated locally excited state (LE) and the highly polar ICT (planar, PICT, or twisted, TICT) state subsequently produced. The study of this peculiar phenomenon has attracted a great deal of attention since its first observation.[2] In particular, the appearance of dual emission is well documented and has been thoroughly investigated in dialkylamino benzonitriles by using stationary and time-resolved fluorescence measurements.[3-5] More recently, the presence of two emitting states has been revealed also in donor-acceptor stilbenes,[6−8] dialkylamino purines[9] and alkylamino lactones.[10] All these neutral push-pull compounds are characterised by a substantial positive fluorosolvatochromism, that is by a large red shift of the emission spectrum in the more polar solvents.[11] Femtosecond resolved spectroscopies have been crucial in order to get a full understanding of the excited state deactivation.[5,6,8,12,13] Particularly, the observation of rise−decay dynamics in the fluorescence up−conversion kinetics and of an isosbestic point in the time−resolved area−normalised emission spectra (TRANES) undoubtedly indicate the presence of two emissive electronic states.[14-16] The careful analysis of the ultrafast fluorescence data has therefore become a valuable tool to distinguish between the occurrence of population transfers (such as proton transfer or ICT) and simple relaxation processes (such as solvation or vibrational cooling), which are usually very difficult to discriminate.

While dual emission and the presence of multiple emitting states are now considered usual phenomena related to the occurrence of ICT in neutral donor-acceptor compounds showing positive fluorosolvatochromism, just few scattered examples of dual emissive ionic or zwitterionic systems showing negative solvatochromism may be found in the literature.[17-20] Indeed, the excited state deactivation of these compounds has been often interpreted considering just the solvent and vibrational relaxation of one electronic state[21-22] and the possible involvement of additional intermediate states is still controversial.[23-24] A push-pull cationic pyridinium salt bearing a dimethylamino phenyl as electron donor portion has recently come to our attention.[25,26] This system has shown a strong negatively solvatochromic behaviour of the absorption spectra and a non-solvatochromic emission band. Nevertheless, femtosecond transient absorption measurements have pointed out that, while the dynamics is solvation controlled in all polar solvents, a longer-lived intermediate species is present in low polar media possibly ascribable to the initially produced electronic state (LE; planar and characterised by a low dipole moment), which subsequently undergoes charge rearrangement in the excited state (slow in these solvents) to produce the fully relaxed S_1 (TICT state; twisted, the twisting concerning the rotation of the methylpiridinium, and characterised by a high dipole moment according to the theoretical calculations).[25]

In the present work, an analogous pyridinium iodide, bearing a stronger electron donor (a diphenylamino group, see Chart 1), has been studied in solvents of different polarity by using not only stationary and transient absorption spectroscopies, but also femtosecond fluorescence up-conversion. This latter, coupled with the investigation of the temperature effect on the emissive properties, has given valuable information about the excited state dynamics of this positively charged dipolar system.

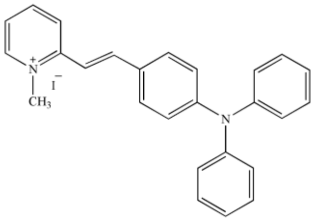

Chart 1. Molecular structure of 2-4-(diphenylamino)phenyl-ethenyl,1-methylpyridinium iodide.

Results and discussion

Absorption spectra of the diphenylamino pyridinium derivative are reported in Figure 1. They show a significant blue shift upon increasing the solvent polarity. A clear correlation of the absorption maximum position with solvent polarity can be seen when alkane chloride and protic solvents are considered (see Table 1), as reported in the literature for another methyl−pyridinium derivative.[27] The absorption properties parallel what previously observed for the dimethylamino analogue and therefore the consequent negative solvatochromism is probably mainly related to the decrease of dipole moment when going from the ground to the first excited singlet state.[25] As to the conformational dynamics, even though in principle the investigated compound may exist in the ground state as equilibrium between two conformers originated from the rotation around the quasi-single bonds between the aryl groups and the double bond, our experimental data (the λ_{exc}-independent emission spectrum and the coincident absorption and fluorescence excitation spectra, Figure S1) indicate that this equilibrium is completely shifted towards one species at room temperature. The emission spectrum behaviour has been found to be very different from the non−solvatochromic one observed for the dimethylamino derivative. In fact, the fluorescence band is slightly blue shifted and significantly enlarged upon increasing the solvent polarity (Figure 1 and Table 1): this apparent broadening may be a hint of the contribution of an additional excited state placed at higher energy to the steady−state emission in the more polar solvents. Fluorescence quantum yields (Table 1) are rather low in all the investigated solvents; they decreased with respect to those of the dimethylamino derivative in the same media[25] pointing to a stronger charge transfer (TICT) character of the excited states, in agreement with the presence of a more efficient electron donor (diphenylamino group). The fluorescence efficiency is quenched by two orders of magnitude on going from the low polar chloroform ($CHCl_3$) to the highly polar water (W). It is thus likely that in W the TICT nature of the fully relaxed S_1 state becomes so important that its deactivation is almost completely non-radiative (by internal conversion) and the very weak emission from an upper excited state becomes detectable.

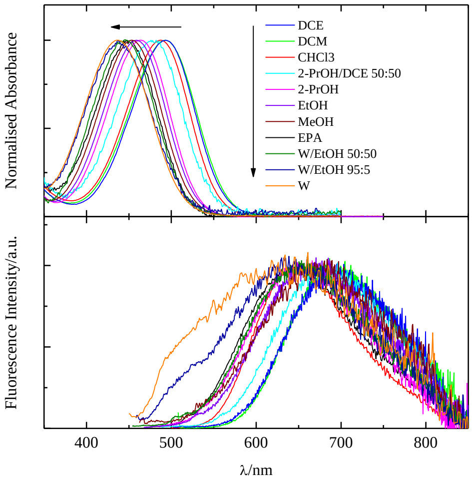

Figure 1. Normalised absorption and emission spectra in solvents of different polarity.

Table 1. Spectral properties and fluorescence quantum yields in solvents of increasing polarity.

Solvent	***f (ε, n²)ᵃ***	λ_{max}^{abs} /nm	λ_{max}^{em} /nm	$\Delta\nu_{s,max}$ /cm^{-1}	**FWHM**$_{abs}$/ cm^{-1}	**FWHM**$_{em}$ /cm^{-1}	ϕ_F
EPA	*0.237*	*450*	*650*	*6720*	*4300*	*3790*	*0.019*
$CHCl_3$	0.296	487	647	5080	3700	3203	0.031
DCM	0.437	491	695	5980	3446	3323	0.026
DCE	0.445	492	693	5900	3660	3494	0.017
2-PrOH/DCE (50:50)	0.498	477	681	6280	4188	3548	0.017
2-PrOH	0.552	464	655	5980	4043	3716	0.054
2-PrOH/EtOH (50:50)	0.564	459	660	6630	4136	3866	0.012
Ac	*0.570*	*448*	*703*	*8100*	*4303*	*3733*	*0.0077*
EtOH	0.577	459	667	6790	4172	3740	0.0063
W/EtOH (30:70)	0.608	446	655	7150	4446	4155	0.0055
MeCN	*0.611*	*447*	*710*	*8290*	*4299*	*3697*	*0.0012*
MeOH	0.617	451	680	7470	4267	4063	0.0023
W/EtOH (50:50)	0.620	445	654	7160	4466	3908	0.0041
W/EtOH (70:30)	0.629	444	663	7440	4931	3953	0.0023
W/EtOH (95:5)	0.637	439	640	7150	5131	4933	0.0008
W	0.640	437	645	7380	4851	6778	0.0003

[a] $f(\varepsilon,n^2)=[2(\varepsilon-1)/(2\varepsilon+1)]-[2(n^2-1)/(2n^2+1)]$. In Italics data referring to non-chlorinated and non-protic solvents.

The peculiarity of the emissive behaviour of this compound pushed us to a deeper investigation, carrying out a study of the temperature effect on the fluorescence in a low polar mixture of solvents (EPA). Emission spectra have been recorded in a wide temperature range below room temperature (normalised spectra are shown in Figure 2). The fluorescence spectrum, which appears broad and centred at 650 nm at 293 K, is strongly blue shifted and narrowed upon decreasing the temperature (Table S1). In a rigid matrix (83 K) the fluorescence maximum is at ~520 nm, in a spectral position corresponding to the shoulder appearing in the emission spectra recorded at room temperature in the highly polar solvents (Figure 1). Moreover, the fluorescence quantum yield results significantly enhanced at low temperatures (see Table S1), reaching a value close to unity at 83 K. These findings suggest that in rigid matrix the population of the relaxed twisted ICT state is inhibited and the emission comes from a more energetic electronic state (LE). The upper emitting state undergoes a fast ICT process at room temperature and a radiative deactivation pathway at low temperature whereas the lower energy ICT state deactivates mainly by internal conversion (the occurrence of competitive *trans−cis* photoisomerisation has been investigated in two solvents of different polarity, $CHCl_3$ and MeCN, and in all cases it has been found to be negligible).

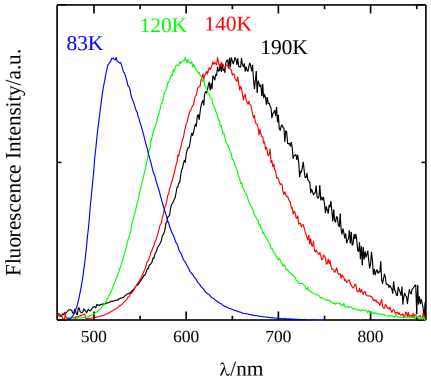

Figure 2. Temperature effect on the emission spectrum in EPA.

From the fluorescence quantum yields at different temperatures an activation (likely torsional) barrier of 2.4 kcal/mol has been determined for the population of the relaxed ICT state in the low polar EPA mixture (see Figure S2). At low temperature the fluorescence intensity increases and the kinetics slows down allowing to determine the fluorescence lifetimes by using a nanosecond resolved single photon counting equipment. The results obtained from the exponential fittings are collected in Table 2. Starting from 190 K and down to 140 K the decay profiles have been well reproduced by mono-exponential functions characterised by a lifetime increasing from 0.95 to 2.5 ns. Nevertheless at 130, 120 and 110 K the fluorescence kinetics have shown a wavelength dependence and in some cases a bi-exponential behaviour. The additional lifetime of about 1.6 ns is associated to a decay in the blue side of the fluorescence spectrum and to a rise in its red side; such experimental evidence indicates that this second emissive component may be the precursor of the longer living one emitting at lower energy. In rigid matrix the fluorescence decay returns to be mono-exponential, pointing out that in this case just one species contributes to the steady-state emission centred at 520 nm.

Table 2. Temperature effect on the fluorescence lifetimes in EPA measured by nanosecond resolved SPC fluorescence spectroscopy (λ_{exc}=460 nm).

T/K	λ_{em}/nm	$\tau_{F,LE}$ /ns	$\tau_{F,ICT}$/ns
190	650		0.95
170	650		1.49
150	650		2.14
140	640		2.51
130	640		2.95
	550	1.64	
120	630	1.40(–)	2.92(+)
	550	1.63(+)	2.60(+)
110	630		2.98(+)
	500	1.66	
78	600	2.47	
	522	2.34	

Femtosecond transient absorption measurements have been carried out by exciting the sample at 400 nm (where the $S_0 \rightarrow S_1$ absorption should be predominant, see Figure 1) in a low polar solvent such as the EPA mixture and in the highly polar W. The time–resolved spectra recorded in both solvents (see panel B of the graphs in Figures S3 and S4) show a broad band of excited state absorption centred around 500 nm and a negative band of stimulated emission red-shifting with time in the spectral range between 550 and 800 nm. The Global and Target Analyses of the acquired data revealed the presence of five and four exponential components in EPA and W respectively, whose lifetimes and Species Associated Spectra (SAS) are shown in Figures S3 and S4, panels C, and summarised in Table 3. The two short components (τ_S=0.52 and 2.5 ps in EPA; τ_S=0.30 and 0.70 ps in W) are assigned to the inertial and diffusive solvation dynamics.[28] The rest component (a transient not decaying in the investigated time window) can be ascribable to the low efficient production of the lowest excited triplet state T_1, expected for this compound.[29] The longer lived component (τ_L=150 ps in EPA and 8.6 ps in W) reflects the presence of the relaxed lowest excited singlet state of ICT or TICT character, whose lifetime is indeed significantly quenched by the increase in solvent polarity. In EPA an additional medium living component (τ_M=21 ps) has been revealed by the fitting procedure. This transient is supposed to be due to the intermediate $^1LE^*$ state reached by light absorption and slowly evolving into the final $^1ICT^*$ state in this low polarity medium. As previously stated for analogous compounds,[25] the $^1LE^* \rightarrow {}^1ICT^*$ transition becomes faster and solvation controlled in the highly polar aqueous solution where this intermediate species is not distinguishable from the transients associated to solvent reorganisation.

In order to get a deeper insight into the nature of this intermediate transient and to gain a clear−cut proof of the possible presence of two emitting excited states, fluorescence up−conversion kinetics have been acquired in a wide spectral range in EPA and W. In EPA (Figure 3, panel B), the kinetics recorded on the blue wavelength side have shown a fast decay occurring within tens of picoseconds and those on the red side a rise taking place on an analogous time scale followed by a slower decay. The reconstructed emission spectra undergo a significant bathochromic shift in time, reaching, at long delay times, a maximum position resembling that of the stationary fluorescence spectrum.

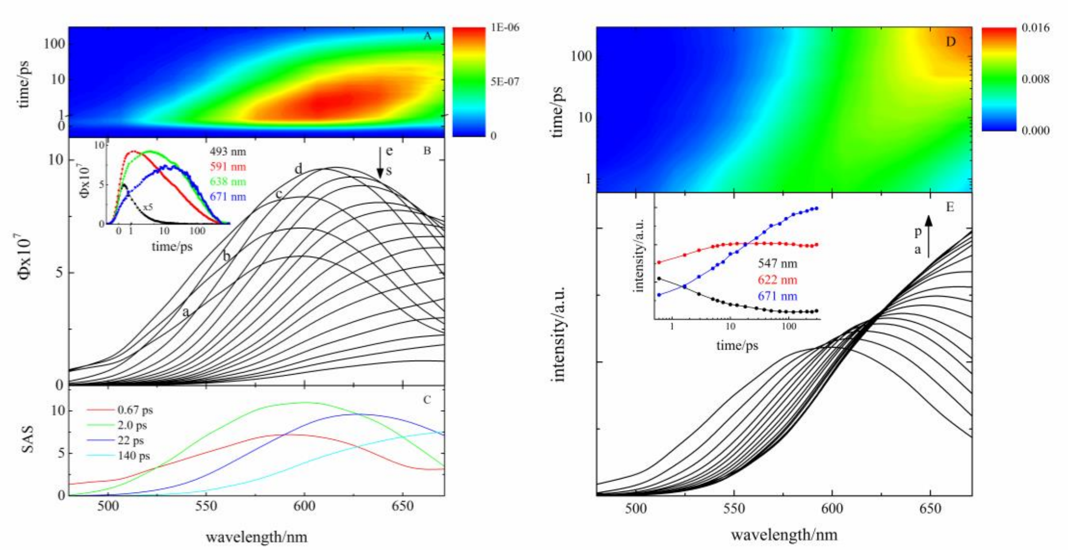

Figure 3. Fluorescence up−conversion (λ_{exc}=400 nm) in EPA. A) contour plot of the experimental data, B) time resolved emission spectra recorded between 0.2 (a) and 300 (s) ps after the laser pulse. Inset: decay kinetics (dots) recorded at meaningful wavelengths together with the corresponding best−fittings (full lines), C) SAS of the decay components obtained by Target Analysis, D) contour plot of the TRANES and E) their spectral evolution recorded between 0.6 (a) and 300 (p) ps after the laser pulse. Inset: time−profiles of TRANES at meaningful wavelengths.

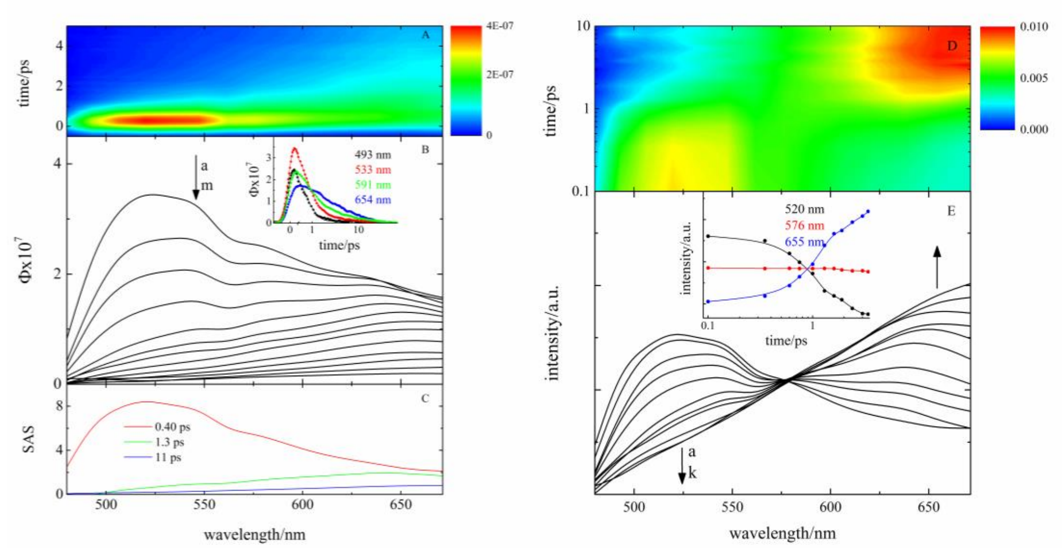

Figure 4. Fluorescence up−conversion (λ_{exc}=400 nm) in W. A) contour plot of the experimental data, B) time resolved emission spectra recorded between 0.35 (a) and 18 (m) ps after the laser pulse. Inset: decay kinetics (dots) recorded at meaningful wavelengths together with the corresponding best−fittings (full lines), C) SAS of the decay components obtained by Target Analysis, D) contour plot of the TRANES and E) their spectral evolution recorded between 0.1 (a) and 3.4 (k) ps after the laser pulse. Inset: time−profiles of the TRANES at meaningful wavelengths.

The global fitting of the acquired data has revealed the presence of the same components already detected during the ultrafast transient absorption investigation (Table 3): the progressive red shift of their SAS maximum would be in agreement with the occurrence of either some relaxation processes or ICT dynamics. However, the TRANES, reported in panel E of Figure 3, show an initial continuous shift toward lower energies (compatible with the solvation dynamics associated to the first two observed transients of 0.67 and 2.0 ps) and an isoemissive point at 622 nm at delays longer than 10 ps (see inset of the aforementioned Figure 3, panel E). This latter is an unambiguous sign of the presence of two emissive electronic states: the LE and ICT states characterised by lifetimes of 22 and 140 ps, respectively, which are the only two species present in solution at delay times longer than 10 ps after light excitation (see Figure 5, panel A).

The emission spectra acquired in W (Figure 4, panel B) exhibit two distinguished bands centred at 520 and 640 nm, respectively, decaying with completely different kinetics. Interestingly, the band at longer wavelengths corresponds to the steady−state fluorescence spectrum, while the one centred at 520 nm recalls the emission detected in the rigid matrix (see Figure 2) and due to the LE state contribution. The dual emissive behaviour is confirmed by a net isosbestic point in the TRANES (Figure 4, panel E), which in this case is already visible looking at the spectra at short delays after the excitation. In fact, in the highly polar W the fast $^1LE^*$ deactivation takes place within the solvation dynamics (described by the exponential components of 0.40 and 1.3 ps, see Table 3) and is thus controlled by it. In the contour plot of the TRANES, the emissions associated to the $^1LE^*$ and $^1ICT^*$ excited states are indeed clearly visible in two well−separated spectral regions.

Table 3. Excited state lifetimes obtained by femtosecond resolved transient absorption (τ_{TA}) and fluorescence up-conversion (τ_{FU}) measurements in EPA and W.

Solvent	τ_{TA}/ps	τ_{FU}/ps	Assignment
EPA	0.52	0.67	$Solv_i$
	2.5	2.0	$Solv_d$
	21	22	$^1LE^*$
	150	140	$^1ICT^*$
	rest		T_1
W	0.30	0.40	$Solv_i$
	0.70	1.3	$Solv_d$
	8.6	11	$^1ICT^*$
	rest		T_1

Experimental

The investigated compound (shown in Chart 1) has been synthesised as iodide salt at the Catania Laboratory following the procedure previously described.[30] Measurements were performed in various solvents: chloroform ($CHCl_3$), dichloromethane (DCM), 1,2-dichloroethane (DCE), acetone (Ac), acetonitrile (MeCN), ethanol (EtOH), methanol (MeOH), 2-propanol (2-PrOH), water (W) and a mixture of 5:5:2 (v/v) isopenthane/diethyl ether/ethanol (EPA).

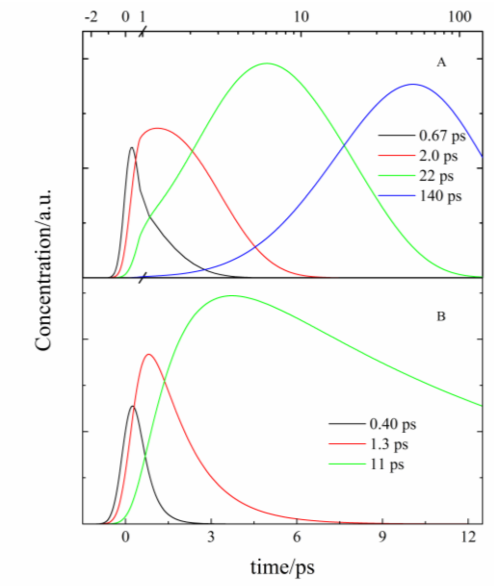

Figure 5. Concentration profiles of the various transients obtained from the Target Analysis of the fluorescence up−conversion data acquired in EPA (panel A) and in W (panel B).

A Cary 4E Varian spectrophotometer was used for the absorption measurements. The fluorescence spectra were measured by a Spex Fluorolog-2 F112AI spectrofluorimeter. Fluorescence lifetimes were measured by an Edinburgh Instrument 199S spectrofluorimeter, using the single photon counting method equipped with a LED source centered at 460 nm, being 0.5 ns the instrumental resolution. Measurements at different temperatures were performed by a cryostat (Oxford Instruments DN 1704). For photochemical measurements, a xenon lamp coupled with an interferential filter (λ_{exc} = 436 nm) and potassium ferrioxalate in 0.1 N sulphuric acid as actinometer were used. The photoreaction (solute concentration ~10^{-4} M) was monitored by HPLC using a Waters apparatus equipped with a Phenomenex Jupiter C18-300Å (4.6 × 250 mm; 5 μm) column and an UV detector. W/MeCN mixtures with 0.1% trifluoroacetic acid were used as eluent. The experimental setups for femtosecond transient absorption and fluorescence up-conversion measurements have been widely described elsewhere.[31-33] Briefly, the 400 nm excitation pulses of ca. 40 fs were generated by an amplified Ti:Sapphire laser system (Spectra Physics). The transient absorption set up (Helios, Ultrafast Systems) is characterised by temporal resolution of ca. 150 fs and spectral resolution of 1.5 nm. Probe pulses were produced in the 475-750 nm range by passing a small portion of 800 nm light through an optical delay line (with a time window of 3200 ps) and focusing it into a 2 mm thick Sapphire window to generate a white-light continuum. In the up-conversion set-up (Halcyone, Ultrafast Systems) the 400 nm pulses excite the sample whereas the remaining fundamental laser beam plays the role of the "optical gate" after passing through a delay line. The fluorescence of the sample is collected and focused onto a BBO crystal together with the delayed fundamental laser beam. The up−converted fluorescence beam is focused into the entrance of a monochromator by a lens, and it is then detected by a photomultiplier connected to a photon counter. The temporal resolution of the up-conversion equipment is about 250 fs, whereas the spectral resolution is 5 nm. Ultrafast spectroscopic data were fitted by Global and Target Analysis using the Glotaran software.[34]

Conclusions

In summary, we have provided straightforward experimental evidence of the occurrence of dual emission in a negatively solvatochromic push−pull cationic system, rarely observed and controversially discussed in the literature. An intermediate species revealed during previous femtosecond transient absorption measurements on analogous methyl pyridinium derivatives pushed us to gain a further insight into the similar excited state dynamics of this salt, which bears a stronger electron donor group and for which an intriguing spectral enlargement has been observed in the stationary fluorescence spectra in highly polar solvents. The investigation of the temperature effect has revealed the presence of two fluorescence lifetimes in the nanosecond range at low temperatures and a significantly blue shifted emission in rigid matrix due to the contribution of an upper excited state. Femtosecond up-conversion kinetics have shown interesting rise−decay dynamics and the reconstructed time resolved spectra have revealed well distinguished emission bands characterised by different deactivations. The detection of a single isoemissive point in the TRANES has unambiguously indicated the presence of two fluorescent excited states (^{1}LE* and ^{1}ICT*) for this donor−acceptor positively charged compound.

Acknowledgements

The authors are grateful to Prof. Ugo Mazzucato for useful discussions and Dr. Fiamma Galletti for some experimental work. The authors thank the Ministero per l'Università e la Ricerca Scientifica e Tecnologica, MIUR (Rome, Italy) [PRIN ''Programmi di Ricerca di Interesse Nazionale'' 2010–2011, no. 2010FM738P and FIRB "Futuro in ricerca" 2013, no. RBFR13PSB6] and Regione Umbria (POR FSE 2007–2013, Risorse CIPE, Perugia, Italy) for fundings.

Notes and references

[a] Department of Chemistry, Biology and Biotechnology and Centro di Eccellenza sui Materiali Innovativi Nanostrutturati (CEMIN), University of Perugia, via Elce di Sotto 8, 06123 Perugia (Italy); email: fausto.elisei@unipg.it.

[b] Department of Chemical Sciences, University of Catania, viale Andrea Doria 6, 95125 Catania (Italy).

Electronic Supplementary Information (ESI) available: Plot of the fluorescence quantum yields at different temperatures according to the Arrhenius-type equation and femtosecond transient absorption data. See DOI: 10.1039/c000000x/

1. Z. R. Grabowski, K. Rotkiewicz and W. Rettig, *Chem. Rev.*, 2003, **103**, 3899.
2. E. Lippert, W. Luder, F. Moll, H. Nagele, H. Boos, H. Prigge and Siebold-Blankestein, *Angew. Chem.*, 1961, **73**, 695.
3. W. Schuddeboom, S. A. Jonker, J. M. Warman, U. Leinhos, W. Kuhnle, K. A. Zachariasse, *J. Phys. Chem.*, 1992, **96**, 10809.
4. K. A. Zachariasse, T. van der Haar, A. Hebercker, U. Leinhos, W. Kuhnle, *Pure & Appl. Chem.*, 1993, **65** (8), 1745.
5. A. Demeter, S. Druzhinin, M. George, E. Haselbach, J. Roulin, K. A. Zachariasse, *Chem. Phys. Lett.*, 2000, **323**, 351.
6. N. Eilers−Konig, T. Kuhne, D. Schwarzer, P. Vohringer, J. Schroeder, *Chem. Phys. Lett.*, 1996, **253**, 69.
7. E. Abraham, J. Oberlè, G. Jonusauskas, R. Lapouyade, C. Rulliere, *Chem. Phys.*, 1997, **214**, 409.
8. D. Pines, E. Pines, W. Rettig, *J. Phys. Chem. A*, 2003, **107**, 236.
9. A. Demeter, S. I. Druzhinin, S. A. Kovalenko, T. A. Senyushkina, K. A. Zachariasse, *J. Phys. Chem. A*, 2011, **115**, 1521.
10. J. Karpiuk, *J. Phys. Chem. A*, 2004, **108**, 11183.
11. B. Carlotti, R. Flamini, I. Kikas, U. Mazzucato, A. Spalletti, *Chem. Phys.*, 2012, **407**, 9.
12. B. Carlotti, R. Flamini, A. Spalletti, F. Elisei, *ChemPhysChem*, 2012, **13** (3), 724.
13. B. Carlotti, I. Kikaš, I. Škorić, A. Spalletti, F. Elisei, *ChemPhysChem*, 2013, **14**, 970.
14. N. Periasamy, A.S.R. Koti, *Proc. Indian Acad. Sci.*, 2003, **69**, 41.
15. L. Gutierrez-Arzaluz, C. A. Guarin, W. Rodrigez-Cordoba, J. Peon, *J. Phys. Chem. B*, 2013, **117**, 12175.
16. M. Park, D. Im, Y. Ho Rhee, T. Joo, *J. Phys. Chem. A*, 2014, **118**, 5125.
17. X. Peng, F. Song, E. Lu, Y. Wang, W. Zhou, J. Fan, Y. Gao, *J. Am. Chem. Soc.*, 2005, **127**, 4170.
18. A. Pigliucci, P. Nikolov, A. Rehaman, L. Gagliardi, C. J. Cramer, E. Vauthey, *J. Phys. Chem. A*, 2006, **110**, 9988.
19. S. Aloise, Z. Pawlowska, C. Ruckebusch, M. Sliwa, J. Dubois, O. Poizat, G. Buntinx, A. Perrier, F. Maurel, P. Jacques, J. Malval, L. Poisson, G. Piani, J. Abe, *Phys. Chem. Chem. Phys.*, 2012, **14**, 1945.
20. B. Wandelt, P. Turkewitsch, B. R. Stranix, G. D. Darling, *J. Chem. Soc. Faraday Trans.*, 1995, **91**, 4199.
21. D. Bingemann, N. P. Ernsting, *J. Chem. Phys.*, 1995, **102**, 2691.
22. A. M. Jonkman, P. Meulen, v.d., H. Zhang, M. Glasbeek, *Chem. Phys. Lett.*, 1996, **256**, 21.
23. B. Strehmel, H. Seifert, W. Rettig, *J. Phys. Chem. B*, 1997, **101**, 2232.
24. R. Ramadass, J. Bereiter-Hajn, *J. Phys. Chem. B*, 2007, **111**, 7681.
25. B. Carlotti, G. Consiglio, F. Elisei, C. G. Fortuna, U. Mazzucato, A. Spalletti, *J. Phys. Chem. A*, 2014, **118**(20), 3580.
26. B. Carlotti, E. Benassi, A. Spalletti, C. G. Fortuna, F. Elisei, V. Barone, *Phys. Chem. Chem. Phys.*, 2014, **16**, 13984.
27. C.-L. Zhan, D. Y. Wang, *J. Photochem. Photobiol. A: Chem.*, 2002, **147**, 93.
28. M. L. Horng, J. A. Gardecki, A. Papazyan, M. Maroncelli, *J. Phys. Chem.*, 1995, **99**, 17311.

29. B. Carlotti, G. Consiglio, F. Elisei, C. G. Fortuna, U. Mazzucato, A. Spalletti, *J. Phys. Chem. A*, 2014, **118** (36), 7782.
30. C.G. Fortuna, V. Barresi, C. Bonaccorso, G. Consiglio, S. Failla, A. Trovato−Salinaro, G. Musumarra, *Eur. J. Med. Chem.*, 2012, **47**, 221 and references therein.
31. A. Barbafina, L. Latterini, B. Carlotti, F. Elisei, *J. Phys. Chem. A*, 2010, **114** (19), 5980.
32. T. Del Giacco, B. Carlotti, S. De Solis, A. Barbafina, F. Elisei, *Phys. Chem. Chem. Phys*., 2010, **12**, 8062.
33. A. Cesaretti, B. Carlotti, P. L. Gentili, C. Clementi, R. Germani, F. Elisei, *J. Phys. Chem. B*, 2014, **118**, 8601.
34. J. J. Snellenburg, S. Laptenok, R. Seger, K. M. Mullen, I. H. M. van Stokkum, *J. Stat. Soft.*, 2012, **49** (3), 1.